Geodesy and Cartography
ISSN 2029-6991 / eISSN 2029-7009
2023 Volume 49 Issue 4: 180–185
https://doi.org/10.3846/gac.2023.18132

UDC 528.94

ESTIMATION OF COASTAL WATERS TURBIDITY USING SENTINEL-2 IMAGERY

Muhammad Anshar AMRAN*, Wasir Samad DAMING

Department of Marine Science, Faculty of Marine Science and Fishery, Hasanuddin University, Makassar, Indonesia

Received 21 November 2022; accepted 22 November 2023

Abstract. Turbidity is an important water quality parameter and an indicator of water pollution. Marine remote sensing techniques has become a useful tool for mapping of turbidity at coastal waters. The advantage of using remote sensing for water quality analysis is its ability to obtain synoptic data from the entire study area to produce continuous surface data, can shows detailed spatial variability and periodically. The empirical modeling has been applied in this study to formulate the mathematical relationship between coastal waters turbidity with Sentinel-2 reflectance. This study integrated field survey and image processing. Measurement of in-situ turbidity was done in accordance with imagery acquisition time. Imageries used for this study were Sentinel-2 level-2A. The mathematical relationship was obtained by multiple linear regression model between turbidity and Sentinel-2 reflectance. A mathematical model has been developed in Sentinel-2 imagery and successfully applied to obtain surface turbidity. Estimated turbidity derived from Sentinel-2 imagery is very close to observed turbidity so the proposed model can be used to retrieve turbidity of coastal waters.

Keywords: coastal waters, turbidity, Sentinel-2, reflectance, empirical modeling, multiple linear regression.

Introduction

Turbidity is an expression of the light-scattering property of water caused by the presence of fine suspended matter such as clay, silt, plankton, and other microscopic organisms. The degree of scattering depends on the amount, size and composition of the suspended matter. Turbidity refers to the decreased ability of water to transmit light caused by suspended particulate matter (Boyd, 2000). Turbidity measurement uses a nephelometry turbidimeter that principally compares light scattering by water samples to standard solutions. The units of turbidity from a calibrated nephelometer are called Nephelometric Turbidity Units (NTU).

Turbidity is one of the indicators of water quality and ecologically important parameter because it is associated with a light limitation for phytoplankton growth. Turbidity distribution can also be used to identify and interpret geomorphological and hydrological processes, such as sediment transport, deposition and resuspension. By identifying the source and spatial distribution of suspended matters, it is possible to deduce relevant spatial information about the availability of essential nutrients in the primary production of coastal waters. The linkage is characterized as a nutrient flow and the reduction of light penetration into the water (Ouillon et al., 2004; Petus et al., 2010; Güttler et al., 2013). Turbidity may endanger fish and other marine organisms by reducing food supplies, destroying spawning areas, and affecting the ability of fish gills to absorb dissolved oxygen. In estuarine waters with high turbidity, dissolved oxygen concentrations can decrease dramatically, which can lead to decline of marine organisms (Gernez et al., 2014; Quang et al., 2017).

Conventional turbidity monitoring requires a large number of in-situ measurement points that are demanding both in time and cost. In addition, traditional methods are constrained by poor spatial and temporal scopes. Alternatively, continuous measurement strategies using point locations with data-loggers can overcome temporal variations in water turbidity at designated locations, but fail to provide synoptic representations of water dynamics. Effective mapping and monitoring of water quality in coastal environments is very difficult due to temporal and spatial variations. Many investigators have been limited by the inability to review a large coastal area as a whole at the same time so that mapping has to be done by relying on data from a series of sampling stations and then interpolating parameter values between stations or extrapolating

*Corresponding author. E-mail: *muhammadansharamran@gmail.com*

to a wider area than the coverage of the station distribution.

In recent years, marine remote sensing techniques has become a useful tool for mapping turbidity at coastal waters. The advantage of using remote sensing for water quality analysis is its ability to obtain synoptic data from the entire study area to produce continuous surface data, can shows detailed spatial variability and periodically. The use of remote sensing technology for monitoring water quality has been carried out by several researchers, and is proven to be a cost-effective method with acceptable accuracy (Brezonik et al., 2007; Islam et al., 2007; Wu et al., 2015; Hu et al., 2016). The studies were to formulate the method of obtaining the quantity of water quality parameters from various sensors (Liu et al., 2003; Brezonik et al., 2005; Islam et al., 2007; Miller et al., 2015; Lihan et al., 2008), that show a similarity in the relationship between water quality parameters and remote sensing data, but the relationship is concluded to be locally specific (Liu et al., 2003; Sravanthi et al., 2013). Satellite remote sensing can be used to study the spatiotemporal variations of surface turbidity, and satellite-derived turbidity maps are useful tools for studying the effect of turbidity in shallow waters (Dogliotti et al., 2015; Quang et al., 2017).

Turbidity mapping and other water quality parameters have been conducted using data from wide-swath ocean color instruments such as SeaWiFS, Aqua/MODIS and ENVISAT/MERIS medium resolution images. For small or narrow areas, however, these applications are mismatched because their low spatial resolution causes many mixed pixels, resulting in low precision estimates. For this case, we can use Sentinel-2 imagery which has a higher spatial resolution of 10 m. Sentinel-2 has been used to analysis of turbidity patterns in coastal lagoon (Sebastiá-Frasquet et al., 2019).

Sentinel-2 consists of a pair of satellites that are part of the European Union's Copernicus Program for observations of the Earth's surface. To cover the full surface of the Earth every 3–5 days, Sentinel-2A and Sentinel-2B are in the same orbit but 180 degrees apart. Sentinel-2 data is categorized according to pre-processing level. Level-0, Level-1A, and Level-1B data are primarily composed of unprocessed raw satellite data. Surface reflectance detected at the top of the atmosphere is categorized as Level-1C. Level-2A is the bottom of atmosphere reflectance is created by applying the Sen2Cor algorithm to Level-1C (Obregón et al., 2019). The best data for research purposes is Level-2A since it enables extra analysis without requiring more atmospheric corrections.

Studies on turbidity distribution using remote sensing technology have been done mostly follow semi-analytic or empirical models that correlate between remote sensing reflectance with field turbidity (Ouillon et al., 2008; Doxaran et al., 2009; Petus et al., 2010; Güttler et al., 2013; Vanhellemont & Ruddick, 2014; Dogliotti et al., 2015; Zhang et al., 2016). Ouma et al. (2020) have used Sentinel-2 (level-1C) to model the relationship between reflectance and turbidity of inland water reservoir. Estimation of turbidity using Sentinel-2 (level-1C) data has also been used by Katlane et al. (2020) in the Gulf of Gabes, Tunisia.

This study aims to create a model to estimate coastal waters turbidity using Sentinel-2A level-2A. The empirical modeling has been applied in this study, which is based on the correlation between reflectance (R) extracted from Sentinel-2 and field measurements. The model has been validated by in-situ observations of turbidity in coastal waters of Makassar, Indonesia.

1. Materials and methods

Remote sensing studies for water quality generally use the preparation of regression models between water reflectance and in-situ quantities of water quality parameters. Regression models were tested on single band reflectance and inter-band ratio. The best model was chosen based on the coefficient of determination (R^2) of the model which was the larger or close to 1. The selected model was applied to Sentinel-2 imagery to map quantitative turbidity in all parts of coastal waters of study area.

The general approach includes (1) taking water samples from predetermined sample locations simultaneously with the overpassing of Sentinel-2 satellite; (2) turbidity measurement of water samples; (3) development of regression models from Sentinel-2 data to estimate turbidity of waters; (4) applying a regression model to map the spatial distribution of water turbidity throughout the study area; and (5) assessment of modeling accuracy.

The study area comprises the coastal waters of Makassar City, Indonesia (Figure 1). There are several locations of turbidity sources in the waters including estuary of Jeneberang River, estuary of Tallo River and Makassar New Port.

This study integrated field survey and image processing. Field surveys include coordinates measurement of the sampling points (using Garmin GPSMap 64S) and measurements of turbidity (using Lutron TU-2016 Turbidimeter) were done in accordance with imagery acquisition time. The measurement points were placed on the region indicating a variation of turbidity. The field survey was carried out four times to create the model and twice to validate the resulting model. The survey is measured at 60 sampling points each time, therefore 240 data are used to build the model, which is subsequently validated with 120 data.

Imageries used for this study were Sentinel-2 level-2A downloaded freely from the Sentinel Scientific Data Hub (https://scihub.copernicus.eu/). The imageries used to build the model were acquired on June 26, 2022, July 13, 2022, July 23, 2022, and July 28, 2022. While the imageries used for validation were obtained on August 22, 2022 and September 1, 2022.

Image correction was done to improve image quality. Geometric correction is performed to put each pixel in the image at the actual coordinates by the first order polynomial transformation method then followed by interpolating pixel values using nearest neighbor resampling.

Correlation test was applied by calculating Pearson's moment-product correlation coefficient meant to know the closely linear relationship between turbidity and Sentinel-2 reflectance. Image bands tested were band-2 (blue band), band-3 (green band), band-4 (red band) and band-8 (NIR band), because electromagnetic radiation can penetrate the water's surface in these wavelengths of the bands. These four bands have a spatial resolution of 10 meters. Reflectance values tested were the reflectance in the single band and the ratio between the bands. The test of inter-band ratio is intended to avoid the reflection effect from the sea bottom. Mathematical relationship was obtained by multiple linear regression model between measurable turbidity and reflectance on the imageries.

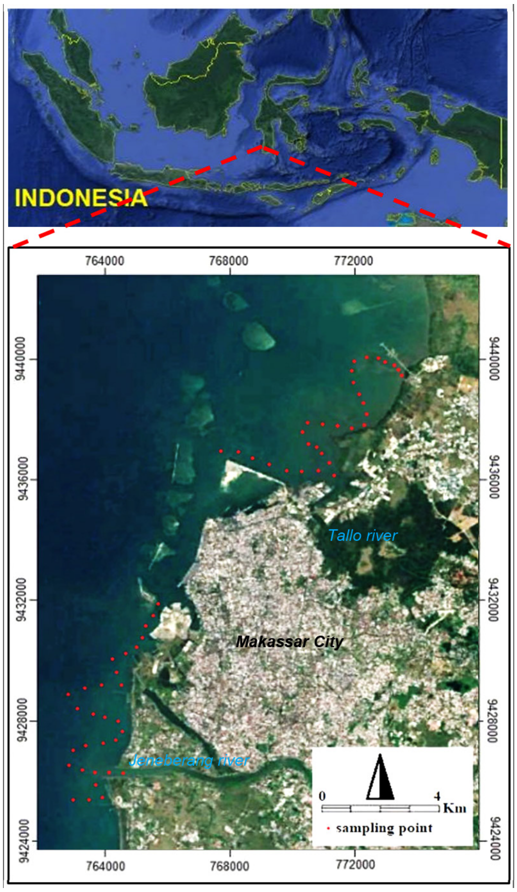

Figure 1. The coastal area of Makassar, Indonesia

Validation is done to determine the accuracy of the model by calculating the root mean square error (RMSerror).

$$RMSerror = \sqrt{\frac{\sum_{i=1}^{n}\left(T_{obs,i} - T_{model,i}\right)^2}{n}}, \quad (1)$$

where: $T_{obs,i}$ – observed (in-situ) turbidity; $T_{model,i}$ – turbidity of model; n – amount of data.

2. Results

Correlation test (Table 1) indicated that high correlation values were obtained on single band of band-3 and band-4, as well as the ratio between bands (band-3/band-2), (band-4/band-2) and (band-8/band-4).

Table 1. Coefficient of correlation (r) between observed turbidity and bands reflectance (R)

Bands reflectance	r
R_2	0.218
R_3	0.637
R_4	0.856
R_8	0.399
R_3/R_2	0.809
R_4/R_2	0.839
R_8/R_4	–0.888

The mathematical relationship was obtained through regression analysis by determining turbidity as dependent variable while correlated reflectance (and reflectance ratio) as independent variables. Stepwise variable selection method was used to optimize the number of involved independent variables. Regression analysis yielded 2 tentative mathematical equations:

$$Turbidity_1 = -3.452 + 10.585\left(\frac{R_3}{R_2}\right) + 18.519\left(\frac{R_4}{R_2}\right) - 23.230\left(\frac{R_8}{R_4}\right); \quad (2)$$

$$Turbidity_2 = -0.304 + 5.305\left(\frac{R_3}{R_2}\right)^2 + 10.283\left(\frac{R_4}{R_2}\right)^2 - 12.939\left(\frac{R_8}{R_4}\right)^2. \quad (3)$$

Both models have the same discriminant coefficient of 0.927. RMSerror test (Table 2) showed that model (2) has the smallest value meaning that the model has the smallest average deviation. Based on the value of R^2 and RMSerror then model $Turbidity_1$ (2) selected to estimate turbidity.

Table 2. Discriminant coefficient (R^2) and RMSerror

Model	R^2	RMSerror
$Turbidity_1$ (2)	0.927	0.189
$Turbidity_2$ (3)	0.927	0.220

Estimated turbidity from this model was very close to in-situ turbidity. Figure 2 showed a very consistent relationship between the estimated turbidity and in-situ turbidity.

The model obtained, $Turbidity_1$, was applied to Sentinel-2 image to produce turbidity distribution maps according to the date of image acquisition (Figure 3).

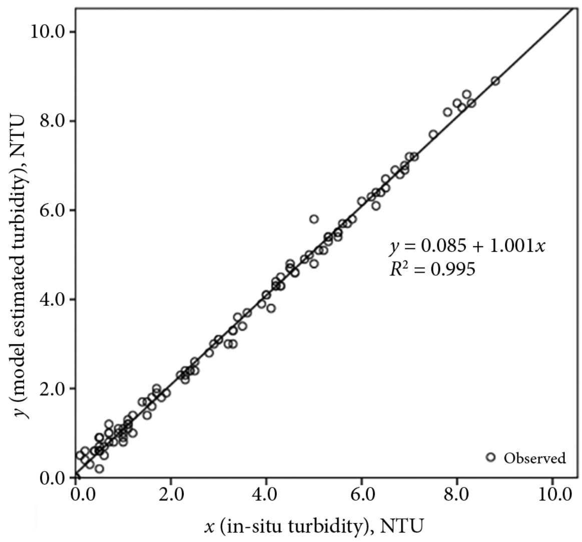

Figure 2. Relationship between estimated and in-situ turbidity

3. Discussion

Significant correlation values of R_3, R_4, (R_3/R_2) and (R_4/R_2) indicate the effect of phytoplankton on turbidity. The chlorophyll of phytoplankton reflect the green spectrum (band-3) and absorb the red and blue spectra (band-4 and band-2). Green band reflectance is highly correlated with low turbidity, whereas red band reflectance is highly correlated with high turbidity (Ouillon et al., 2004). Research in estuarine of Matla, Bay of Bengal, India, also shows that turbidity is closely related to the reflectance of green bands and red bands (Ray et al., 2013). The high correlation coefficient in the red band is in accordance with the results obtained by Katlane et al. (2020).

The correlation value of (R_8/R_4) is also high indicating the effect of suspended sediment on turbidity. Band-8 and band-4 on Sentinel-2 are sensitive to the presence of soil elements. This means that turbidity in the study area is also affected by suspended sediments. The dynamics

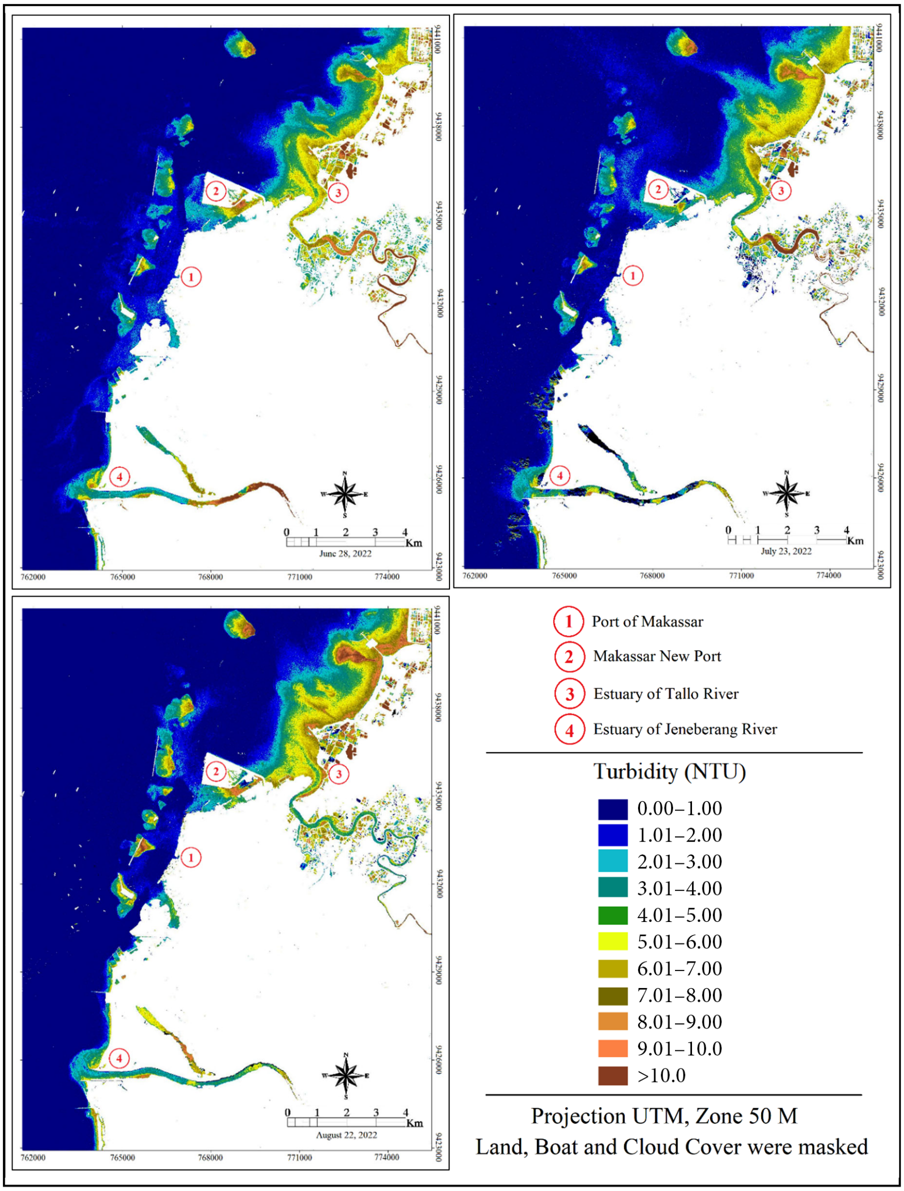

Figure 3. Distributions of estimated turbidity were derived from Sentinel-2

of sediments produced by wave erosion, tidal currents, hydrological parameters, biological and chemical components of water all affect the shallow water areas along the coast and in estuaries (Katlane et al., 2020). Band-8 (NIR) is used to avoid reflected radiation from the bottom of the water. In order to avoid significant interference from the bottom, it is necessary to measure turbidity in shallow waters using spectral bands that are sensitive to turbidity and have a restricted depth penetration (Caballero et al., 2019). Rapid increases in water absorption are observed from red to NIR. Absorption in this spectrum limits radiation from the bottom but scatters radiation from suspended particles. A nice balance between turbidity detection and bottom detection is provided by these bands.

Increased turbidity always increases the energy flux that reaches the sensor, because more solar energy is reflected or backscattered by suspended particles in the water. If the suspended particle were phytoplankton or microalgae, the scattering energy was in the visible spectrum, especially in the green band. Whereas if the suspended particle is a soil particle, the scattering energy tends to red and near infrared spectrum. The use of red and near infrared bands in turbidity mapping using remote sensing imagery has been demonstrated in the model prepared by Dogliotti et al. (2015). The visible spectrum is sensitive to turbidity, while the near infrared spectrum is also sensitive to turbidity even better than the visible spectrum because it is less influenced by bottom reflectance in shallow waters. Suspended particles increase total scattering, increase backscattering, change the spectral distribution of light, and reduce the average path length. The most important result of this effect is that turbid water is more reflective than clear water at all visible and near infrared wavelengths.

The produced maps show spatio-temporal variations in water turbidity. Validation through the determination coefficient and RMSerror shows that the model has confirmed the potential use of satellite imagery for mapping coastal waters turbidity. However, to map water turbidity in estuary areas, it is necessary to use finer imagery resolution and more ground-truth due to the highly turbidity variation.

$Turbidity_1$ model applied to the Sentinel-2 produces turbidity distribution maps (Figure 3). The maps show the high turbidity at Jeneberang estuary, area of the Makassar New Port, Tallo estuary and the northern coastal area of Tallo estuary. The high turbidity in the Jeneberang and Tallo estuary were due to a large flow of turbid water from the river into estuary. Turbidity around the Makassar New Port is caused by reclamation activities that adding piles of soil to coastal waters. The high turbidity in the northern shallow coastal waters of Tallo estuary is mainly due to sediment re-suspension. Re-suspension is easy in this section because the waters are shallow, the beach profile is flat and the sediments are fine sand and very fine sand, so that even with small waves and slow currents it can stir up the sediment. The high turbidity in all four parts of the regions also illustrates the high concentration of suspended sediment in the waters. Suspended sediments are rich in nutrients and are considered to be the cause of eutrophication. So, it is very important to have a time series record of turbidity for a better understanding of land-sea interactions because it negatively affects to aquaculture and is dangerous for benthic invertebrates.

Conclusions

This study produced a model to estimate turbidity using remote sensing data. A mathematical model has been developed in Sentinel-2 level-2A imagery and successfully applied to obtain coastal waters turbidity. Estimated turbidity derived from Sentinel-2 imagery is very close to observed turbidity. This indicates that the proposed model can be used to obtain turbidity of coastal waters. The results of this study can be used as a reference for monitoring the pattern of turbidity distribution and can also be applied to similar coastal waters.

References

Boyd, C. E. (2000). *Water quality: An introduction*. Springer Science+Business Media. https://doi.org/10.1007/978-1-4615-4485-2_1

Brezonik, P., Menken, K. D., & Bauer, M. (2005). Landsat-based remote sensing of lake water quality characteristics, including chlorophyll and colored dissolved organic matter (CDOM). *Lake and Reservoir Management*, *21*(4), 373–382. https://doi.org/10.1080/07438140509354442

Brezonik, P. L., Olmanson, L. G., Bauer, M. E., & Kloiber, S. M. (2007). Measuring water clarity and quality in Minnesota lakes and rivers: A census-based approach using remote-sensing techniques. *Cura Reporter*, *37*, 3–13.

Caballero, I., Stumpf, R. P., & Meredith, A. (2019). Preliminary assessment of turbidity and chlorophyll impact on bathymetry derived from Sentinel-2A and Sentinel-3A satellites in South Florida. *Remote Sensing*, *11*(6), 645. https://doi.org/10.3390/rs11060645

Dogliotti, A. I., Ruddick, K. G., Nechad, B., Doxaran, D., & Knaeps, E. (2015). A single algorithm to retrieve turbidity from remotely-sensed data in all coastal and estuarine waters. *Remote Sensing of Environment*, *156*, 157–168. https://doi.org/10.1016/j.rse.2014.09.020

Doxaran, D., Froidefond, J. M., Castaing, P., & Babin, M. (2009). Dynamics of the turbidity maximum zone in a macrotidal estuary (the Gironde, France): Observations from field and MODIS satellite data. *Estuarine, Coastal and Shelf Science*, *81*(3), 321–332. https://doi.org/10.1016/j.ecss.2008.11.013

Gernez, P., Barille, L., Lerouxel, A., Mazeran, C., Lucas, A., & Doxaran, D. (2014). Remote sensing of suspended particulate matter in turbid oyster-farming ecosystems. *Journal of Geophysical Research: Oceans*, *119*(10), 7277–7294. https://doi.org/10.1002/2014JC010055

Güttler, F. N., Niculescu, S., & Gohin, F. (2013). Turbidity retrieval and monitoring of Danube Delta waters using multi-sensor optical remote sensing data: An integrated view from the delta plain lakes to the western–northwestern Black Sea coastal zone. *Remote Sensing of Environment*, *132*(15), 86–101. https://doi.org/10.1016/j.rse.2013.01.009

Hu, Z., Pan, D., He, X., & Bai, Y. (2016). Diurnal variability of turbidity fronts observed by geostationary satellite ocean color remote sensing. *Remote Sensing*, *8*(2), 147–162. https://doi.org/10.3390/rs8020147

Islam, M. A., Lan-Wei, W., Smith, C. J., Reddy, S., Lewis, A., & Smith, A. (2007). Evaluation of satellite remote sensing for operational monitoring of sediment plumes produced by dredging at hay point, Queensland, Australia. *Journal of Applied Remote Sensing*, *1*(1), 011506–011521. https://doi.org/10.1117/1.2834768

Katlane, R., Dupouy, C., El Kilani, B., & Berges, J. C. (2020). Estimation of chlorophyll and turbidity using Sentinel 2A and EO1 data in Kneiss Archipelago Gulf of Gabes, Tunisia. *International Journal of Geosciences*, *11*, 708–728. https://doi.org/10.4236/ijg.2020.1110035

Lihan, T., Saitoh, S. I., Iida, T., Hirawake, T., & Iida, K. (2008). Satellite-measured temporal and spatial variability of the Tokachi River plume. *Estuarine Coastal and Shelf Science*, *78*(2), 237–249. https://doi.org/10.1016/j.ecss.2007.12.001

Liu, Y., Islam, M. A., & Gao, J. (2003). Quantification of shallow water quality parameters by means of remote sensing. *Progress in Physical Geography*, *27*(1), 24–43. https://doi.org/10.1191/0309133303pp357ra

Miller, P. I., Xu, W., & Carruthers, M. (2015). Seasonal shelf-sea front mapping using satellite ocean colour and temperature to support development of a marine protected area network. *Deep-Sea Researh Part II-Topical Study in Oceanography*, *119*, 3–19. https://doi.org/10.1016/j.dsr2.2014.05.013

Obregón, M. A., Rodrigues, G., Costa, M. J., Potes, M., & Silva, A. M. (2019). Validation of ESA Sentinel-2 L2A aerosol optical thickness and columnar water vapour during 2017–2018. *Remote Sensing*, *11*(14), 1649. https://doi.org/10.3390/rs11141649

Ouillon, S., Douillet, P., & Andrefouet, S. (2004). Coupling satellite data with in situ measurements and numerical modeling to study fine suspended-sediment transport: A study for the lagoon of New Caledonia. *Coral Reefs*, *23*(1), 109–122. https://doi.org/10.1007/s00338-003-0352-z

Ouillon, S., Douillet, P., Petrenko, A., Neveux, J., Dupouy, C., Froidefond, J. M., Andréfouët, S., & Caravaca, A. M. (2008). Optical algorithms at satellite wavelengths for total suspended matter in tropical coastal waters. *Sensors*, *8*(7), 4165–4185. https://doi.org/10.3390/s8074165

Ouma, Y. O., Noor, K., & Herbert, K. (2020). Modelling reservoir chlorophyll-a, TSS, and turbidity using Sentinel-2A MSI and Landsat-8 OLI satellite sensors with empirical multivariate regression. *Journal of Sensors*, *2020*, 8858408. https://doi.org/10.1155/2020/8858408

Petus, C., Chust, G., Gohin, F., Doxaran, D., Froidefond, J. M., & Sagarminaga, Y. (2010). Estimating turbidity and total suspended matter in the Adour River plume (South Bay of Biscay) using MODIS 250-m imagery. *Continental Shelf Research*, *30*(5), 379–392. https://doi.org/10.1016/j.csr.2009.12.007

Quang, N. H., Sasaki, J., Higa, H., & Huan, N. H. (2017). Spatiotemporal variation of turbidity based on Landsat 8 OLI in Cam Ranh Bay and Thuy Trieu Lagoon, Vietnam. *Water*, *9*(8), 570–594. https://doi.org/10.3390/w9080570

Ray, R., Mandal, S., & Dhara, A. (2013). Environmental monitoring of estuaries: Estimating and mapping various environmental indicators in Matla estuarine complex, using Landsat TM digital data. *International Journal of Geomatics and Geosciences*, *3*(3), 570–581.

Sebastiá-Frasquet, M. T., Aguilar-Maldonado, J. A., Santamaría-Del-Ángel, E., & Estornell, J. (2019). Sentinel 2 analysis of turbidity patterns in a coastal lagoon. *Remote Sensing*, *11*(24), 2926. https://doi.org/10.3390/rs11242926

Sravanthi, N., Ramana, I. V., Yunus Ali, P., Ashraf, M., Ali, M. M., & Narayana, A. C. (2013). An algorithm for estimating suspended sediment concentrations in the coastal waters of India using remotely sensed reflectance and its application to coastal environments. *International Journal of Environmental Research*, *7*(4), 841–850.

Vanhellemont, Q., & Ruddick, K. (2014). Turbid wakes associated with offshore wind turbines observed with Landsat 8. *Remote Sensing of Environment*, *145*, 105–115. https://doi.org/10.1016/j.rse.2014.01.009

Wu, G., Cui, L., Liu, L., Chen, F., Fei, T., & Liu, Y. (2015). Statistical model development and estimation of suspended particulate matter concentrations with Landsat 8 OLI images of Dongting Lake, China. *International Journal of Remote Sensing*, *36*(1), 343–360. https://doi.org/10.1080/01431161.2014.995273

Zhang, Y., Zhang, Y., Shi, K., Zha, Y., Zhou, Y., & Liu, M. (2016). A Landsat 8 OLI-based, semianalytical model for estimating the total suspended matter concentration in the slightly turbid Xin'anjiang reservoir (China). *IEEE Journal of Selected Topics in Applied Earth Observations and Remote Sensing*, *9*(1), 1–16. https://doi.org/10.1109/JSTARS.2015.2509469